

Production of Highly Polarized Positron Beams via Helicity Transfer from Polarized Electrons in a Strong Laser Field

Yan-Fei Li,^{1,*} Yue-Yue Chen,^{2,†} Wei-Min Wang,^{3,4,5} and Hua-Si Hu^{1,‡}

¹*Department of Nuclear Science and Technology, Xi'an Jiaotong University, Xi'an 710049, China*

²*Department of Physics, Shanghai Normal University, Shanghai 200234, China*

³*Department of Physics and Beijing Key Laboratory of Opto-electronic Functional*

Materials and Micro-nano Devices, Renmin University of China, Beijing 100872, China

⁴*Beijing National Laboratory for Condensed Matter Physics, Institute of Physics, CAS, Beijing 100190, China*

⁵*Collaborative Innovation Center of IFSA (CICIFSA),
Shanghai Jiao Tong University, Shanghai 200240, China*

(Dated: March 4, 2020)

The production of a highly-polarized positron beam via nonlinear Breit-Wheeler processes during the interaction of an ultraintense circularly polarized laser pulse with a longitudinally spin-polarized ultrarelativistic electron beam is investigated theoretically. A new Monte Carlo method employing fully spin-resolved quantum probabilities is developed under the local constant field approximation to include three-dimensional polarizations effects in strong laser fields. The produced positrons are longitudinally polarized through polarization transferred from the polarized electrons by the medium of high-energy photons. The polarization transfer efficiency can approach 100% for the energetic positrons moving at smaller deflection angles. This method simplifies the post-selection procedure to generate high-quality positrons in further applications. In a feasible scenario, a highly polarized (40% – 65%), intense ($10^5/\text{bunch}$ – $10^6/\text{bunch}$), collimated (5mrad–70 mrad) positron beam can be obtained in a femtosecond timescale. The longitudinally polarized positron sources are desirable for applications in high-energy physics and material science .

As a powerful probe, spin-polarized positrons play irreplaceable roles in fundamental physical studies and applications. Low-energy (eV to keV) positrons can be utilized to probe the surface [1] and bulk [2] magnetism of materials [3]. High-energy (GeV to hundreds of GeV) positrons improve the sensitivity of the two photon effect experiments [4], and are essential for an unambiguous determination of the nucleon structure [5], testing Standard Model and searching for new physics beyond it [6]. The proposed International Linear Collider (ILC) [7] is designed for discovering physics beyond the Standard Model with polarized electrons and positrons at energies of 500 GeV. The positrons are required with polarization more than 30%, density $\sim 10^{10}e^+/\text{bunch}$, and beam size in nm scale at the interaction point [8].

Polarized positrons can be obtained from beta decays of specific radioisotopes [9]. However, the large angular divergence, large energy spread and low intensity of the positron beam from beta decays limit its applications. Storage rings can be used to polarized positrons via Sokolov-Ternov effect [10], but this time consuming mechanism brings forward rigorous requirements on space scale and layout to experiments. Nowadays, two methods based on BH process are extensively adopted to produce polarized positrons. One is photon-solid interaction, with circularly polarized (CP) γ rays generated by linear Compton scattering between CP lasers with unpolarized electrons [11], or by synchrotron radiation of unpolarized electrons moving in helical undulators [12]. The other is electron-solid interaction, with longitudinally spin-polarized (LSP) electrons [13]. However, the energy conversion efficiency from initial

electrons to photons in the former way is rather low due to the low fundamental parameter $K(\ll 1)$ of the undulator [14]. The latter suffers from high depolarization rates and large angular divergences due to multiple scattering in the Coulomb field of nuclei (Mott scattering) [15, 16], restricting the target thickness to be less than $0.2L_{rad}$ (L_{rad} is the radiation length typically in several mm[17]), and consequently limiting the total yield of positrons to $\lesssim 0.01e^+/e^-$ [13, 15, 18]. Currently, the state-of-the-art techniques can provide polarized positron beams with polarization 30% \sim 80%, density $\sim 10^4e^+/\text{bunch}$, and angular divergence more than 20 degree [11–13, 19]. Challenging technology upgrades are still needed to meet the experimental requirements above [7, 8].

Recent progress in development of ultraintense laser system [20] has stimulated the interest in producing polarized positrons with strong laser field [21–30]. Since the fierce laser-induced pair production is free from Mott scattering and implemented in nonlinear QED regime ($K \gg 1$), the produced positrons are expected to be a desirable alternative along with outstanding features similar with other laser-driven sources [14, 31–33], such as high brilliance [34, 35], ultrashort duration [36], low angular divergence[37] and high beam intensity [38, 39]. For instance, an asymmetric two-color laser field can produce polarized positrons with a polarization degree of around 60%, angular divergence of ~ 74 mrad and yield of $\sim 0.01e^+/e^-$ [27]. Meanwhile, a fine-tuning small ellipticity of a laser pulse results in an angular dependent polarization of created positrons [28]. However, all suggested schemes are only able to deliver positrons with transverse polarization, while longitudinal polarization are employed in most applications. To solve this problem, a polarization rotator has to be applied under the risk of particle-amount plummeting since the rotator works for monoenergetic particles with a limited energy range [40, 41]. Besides, the effect of photon polarization on pair

* liyanfei@xjtu.edu.cn

† yueyuechen@shnu.edu.cn

‡ huasi.hu@mail.xjtu.edu.cn

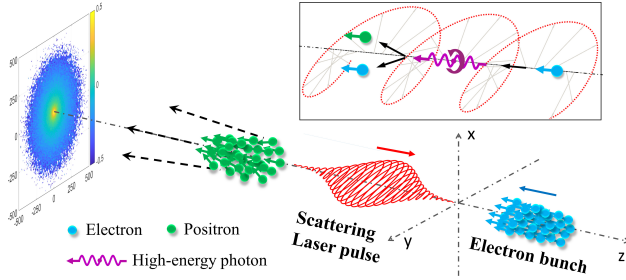


FIG. 1. Scenarios of generation of a LSP ultrarelativistic positron beam via an ultraintense laser pulse head-on colliding with a counterpropagating LSP electron beam. First, longitudinal polarization (helicity) is transferred from electron to photon during NCS, then, from high-energy photon to positron through NBW process, as shown in the inset.

production is not considered in these schemes.

In this letter, we investigate theoretically the feasibility of production of a longitudinally polarized ultrarelativistic positron beam via the interaction of a CP ultraintense laser pulse with a LSP counterpropagating ultrarelativistic electron beam in the quantum radiation-dominated regime [42], see Fig. 1. Two steps contribute to the positron polarization. Firstly, circularly polarized photons are radiated during nonlinear Compton scattering (NCS) of a CP laser pulse with a LSP electron beam [26]. Then, the helicity of the high-energy photons transfers to electron-positron pairs via nonlinear Breit-Wheeler (NBW) pair production process. To self-consistently incorporate the two processes, a new Monte Carlo for the first time involving all polarization effects from electron (positron) and photon in realistic tightly-focused laser fields, is developed for simulations. Our simulation shows, under the external electromagnetic fields, a highly polarized intense positron beam can be produced with a small angular divergence.

Our Monte Carlo method [43–49], treats photon emission and pair production quantum mechanically, and describes the electron (positron) spin-resolved dynamics semiclassically. In particular, photon emission and pair production are conducted by the common statistical event generators, based on quantum probabilities derived via the QED operator method in the local constant field approximation (LCFA) [45], to determine whether or not a photon emission or pair production occurs at each simulation step (see the details in the Supplemental Material [50]). The LCFA is valid in an ultraintense laser fields, with the invariant laser field parameter $a_0 \equiv eE_0/(m\omega_0) \gg 1$, where the formation length of radiation and pair production are far shorter than the laser wavelength and the typical size of the electron (positron) trajectory [43, 45, 51]. Here, E_0 is the laser field amplitude, ω_0 is the laser frequency, and $e(>0), m$ are the electron charge and mass, respectively. Relativistic units $\hbar = c = 1$ are used throughout.

Moreover, our Monte Carlo algorithm features the description of polarization effects. In contrast with the previous Monte Carlo methods related to particular observable of interest [22, 23, 25–28], our new method extends the simulation capacity from solving one-dimensional polarization problem to three-dimensional, by choosing the instantaneous spin quanti-

zation axis (SQA) according to the properties of the scattering process [52] instead of the detector (e.g. the direction of magnetic field in the rest frame [22, 23, 25, 27, 28] or the direction of initial electron polarization [26]). The shortcomings of the previous methods stemming from neglecting the phase relation between the two components of the spinor can be overcome [50]. Meanwhile, since photon polarization significantly affects pair production rate ($\geq 10\%$, investigated recently in [53, 54]) and positron polarization ($\sim 60\%$, see [50]), we improved the Monte-Carlo method [27, 28, 46, 47, 49, 53, 54] by employing the photon-polarization- and pair-spin-resolved pair production probability applicable to strong laser fields [45], and therefore provide a more thorough way to simulate NBW process.

The details of our Monte Carlo algorithm are elaborated as follow. The electron (positron) spin jumps into one of its basis states defined with respect to SQA in each time step, regardless whether a photon emission happens or not. The spin-resolved radiation probability can be written in form of $W_R = a + \mathbf{S}_f^R \cdot \mathbf{b}$ [22, 50]. When a photon emitted, the SQA is chosen to be along \mathbf{b} . The final polarization vector \mathbf{S}_f^R is decided with a stochastic procedure: if $W_R^+/(W_R^+ + W_R^-) > R_a$, $\mathbf{S}_f^R = +\mathbf{b}/|\mathbf{b}|$; otherwise $\mathbf{S}_f^R = -\mathbf{b}/|\mathbf{b}|$. Here, R_a is a random number in $[0,1]$; and W_R^{\pm} are the probabilities calculated by taking \mathbf{S}_f^R as $\pm\mathbf{b}/|\mathbf{b}|$, respectively. When a photon emission does not occur, the electron (positron) spin should also change quantum mechanically [49]. The probability for no photon emission takes the form of $W_{NR} = \frac{1}{2}(c + \mathbf{S}_f^{NR} \cdot \mathbf{d})$ [49], and the SQA is along \mathbf{d} . The final polarization vector \mathbf{S}_f^{NR} is decided with probability W_{NR} and the stochastic procedure mentioned above. Here, a, \mathbf{b}, c and \mathbf{d} are functions of emitted photon energy, field strength and etc [50]. The polarization of the emitted photon is determined with a same algorithm [26, 50].

Similarly, the polarization vectors of a newly created pair is calculated with spin-resolved probability of [45]

$$\frac{d^2 W_{pair}}{d\varepsilon_+ dt} = \frac{C_p}{2} (h + \mathbf{S}_+ \cdot \mathbf{j}), \quad (1)$$

$$h = \left(\frac{\omega_\gamma^2}{\varepsilon_+ \varepsilon_-} - 2 \right) K_{\frac{2}{3}}(\rho) + \text{Int} K_{\frac{1}{3}}(\rho) - \xi_3 K_{\frac{2}{3}}(\rho), \quad (2)$$

$$\begin{aligned} \mathbf{j} = & -\xi_1 \frac{\omega_\gamma}{\varepsilon_-} K_{\frac{1}{3}}(\rho) \hat{\mathbf{e}}_1 - K_{\frac{1}{3}}(\rho) \left(\frac{\omega_\gamma}{\varepsilon_+} - \xi_3 \frac{\omega_\gamma}{\varepsilon_-} \right) \hat{\mathbf{e}}_2 \\ & + \xi_2 \left[\frac{\omega_\gamma}{\varepsilon_+} \text{Int} K_{\frac{1}{3}}(\rho) + \frac{\varepsilon_+^2 - \varepsilon_-^2}{\varepsilon_+ \varepsilon_-} K_{\frac{2}{3}}(\rho) \right] \hat{\mathbf{e}}_v \end{aligned} \quad (3)$$

where $C_p = \alpha m^2 / (\sqrt{3} \pi \omega_\gamma)$; $\omega_\gamma, \varepsilon_+$ and ε_- are the energies of the photon, positron and electron, respectively, with $\omega_\gamma = \varepsilon_+ + \varepsilon_-$; $\rho = 2\omega_\gamma^2 / (3\chi_\gamma \varepsilon_+ \varepsilon_-)$; $\xi = (\xi_1, \xi_2, \xi_3)$ refers to the photon polarization vector with ξ_i ($i = 1, 2, 3$) the Stokes parameters defined with respect to the axes of $\hat{\mathbf{e}}_1$ and $\hat{\mathbf{e}}_2$ [16]; $\hat{\mathbf{e}}_1$ is the unit vector along the direction of the transverse component of acceleration, $\hat{\mathbf{e}}_2 = \hat{\mathbf{e}}_v \times \hat{\mathbf{e}}_1$ with $\hat{\mathbf{e}}_v$ the unit vector along positron velocity. Quantum parameter is defined as $\chi_{\gamma,e} \equiv |e| \sqrt{-(F_{\mu\nu} p^\nu)^2} / m^3$ with p^ν the four-vector of photon or electron (positron) momentum. The spin state of the newborn positron is set as one of the two states: $\mathbf{S}_+ = \pm \mathbf{j}/|\mathbf{j}|$, via

stochastic procedure. The spin state of produced electron is also obtained with Eq.(1), through replacing ε_+ , ε_- and \mathbf{S}_+ with ε_- , ε_+ and \mathbf{S}_- , respectively.

Between quantum events, the electron (positron) dynamics in the ultraintense laser field are described by Lorentz equations classically, and the spin precession is governed by the Thomas-Bargmann-Michel-Telegdi equation [55]. The detailed description and accuracy of the method are exhibited in the Supplemental Material [50].

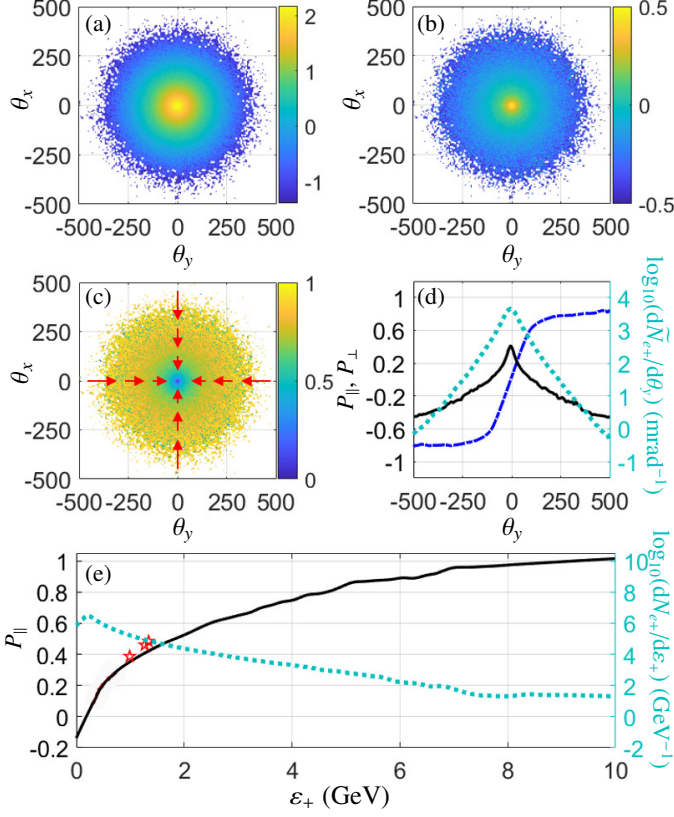


FIG. 2. Angular distribution of number density $\log_{10}(d^2 N_{e+}/d\theta_x d\theta_y)$ (mrad^{-2}) (a), longitudinal polarization $P_{||} = -\bar{S}_z$ (b), and transverse polarization degree $|P_{\perp}| = \sqrt{\bar{S}_x^2 + \bar{S}_y^2}$ (c), vs deflection angles of $\theta_x = p_x/p_z$ and $\theta_y = p_y/p_z$. (d) $P_{||}$ (black-solid), transverse polarization of $P_{\perp} = \bar{S}_y$ (blue-dash-dotted) and positron number density $\log_{10}(d\tilde{N}_{e+}/d\theta_y)$ (mrad^{-1}) (cyan-dotted) vs θ_y . Here, $d\tilde{N}_{e+}/d\theta_y = \int_{-20}^{20} d^2 N_{e+}/(d\theta_x d\theta_y) d\theta_x$. (e) $P_{||}$ (black-solid line) and $\log_{10}(dN_{e+}/d\varepsilon_+)$ (GeV^{-1}) (cyan-dotted line) vs positron-energy ε_+ . The red stars indicate positrons with deflection angle $\theta = \sqrt{\theta_x^2 + \theta_y^2}$ within 5 mrad, 10 mrad, and 20 mrad, from right to left, respectively.

A typical simulation result for production of polarized positrons with a realistic tightly-focused Gaussian laser pulse [56] is shown in Fig.2. The peak laser intensity is $I_0 \approx 2.75 \times 10^{22} \text{ W/cm}^2$ ($a_0 = 100\sqrt{2}$), pulse duration (the full width at half maximum, FWHM) $\tau = 5T_0$ with T_0 the period, wavelength $\lambda = 1\mu\text{m}$, and focal radius $w_0 = 5\lambda$. The colliding electron bunch is set with features of laser-accelerated electron source [31, 57, 58]. $N_e = 9.6 \times 10^5$ electrons uniformly distributed longitudinally and normally distributed transversely

in a cylindrical form at length of $L_e = 6\lambda$ and standard deviation of $\sigma_{x,y} = 0.6\lambda$. The initial mean kinetic energy is 10 GeV, the energy spread 6%, and the angular divergence 0.2 mrad. The case of a longer electron bunch from traditional accelerators is also considered [50]. With the present available electron energy close to 10 GeV by laser wakefield accelerators [57] and hundreds of GeV by traditional accelerators [59], the laser intensity and electron energy are chosen above to keep $\chi_{\gamma,e}^{max} \approx 5.9 \times 10^{-6} a_0 \gamma_e \gtrsim 1$ for substantial high-energy photon emission and pair production. The initial electrons are set to be 100% longitudinally polarized, i.e. $S_z = -1$, for a more visible description on polarization transferring (See [50] for a more relaxed requirement).

The produced positrons mainly concentrate in the center of the angular distribution with angular divergence (FWHM) around 70 mrad, see Figs.2(a). The total yield of positrons is $1.17 e^+/e^-$. Positrons are longitudinally polarized with $P_{||} > 0$ for $\theta \lesssim 250$ mrad and $P_{||} < 0$ for $\theta \gtrsim 250$ mrad, as shown in Figs.2(b). For more intuitive features, one can refer to the angular distribution of density and polarization for positrons at $\theta_x \in [-20, 20]$ mrad, see Fig.2(d). The positron density dramatically declines with the increase of deflection angle; and $P_{||}$ decreases with the rising of $|\theta_y|$, from 43% to -45%. Moreover, $P_{||}$ is proportional to positron energy, similar with that in BH process [18], see Fig.2(e), but the positron yield is two orders higher. Higher polarization can be achieved by using post-selection technique. For instance, for positrons with energy higher than 2 GeV, 4 GeV, 6 GeV, and 8 GeV, polarization degrees are 62.5%, 81.9%, 91.8% and 98.6%, respectively, and the corresponding yields are $0.019 e^+/e^-$, $0.002 e^+/e^-$, $1.51 \times 10^{-4} e^+/e^-$, and $5.21 \times 10^{-6} e^+/e^-$, respectively. The positron energy ranges from MeV to 10 GeV with a mean value of 0.345 GeV, see Fig.2(e). The maximal energy conversion efficiency $\epsilon_{max} \approx 1$ and the average energy conversion efficiency $\bar{\epsilon} \approx 0.034$, much higher than that in BH process ($\epsilon_{max} \approx 0.05$ and $\bar{\epsilon} \approx 0.003$ for photons from linear Compton scattering [11], and $\epsilon_{max} \approx 2 \times 10^{-4}$ and $\bar{\epsilon} \approx 4 \times 10^{-5}$ for photons emitted from a electron beam passing through a helical undulator [60]). Besides, the angle-dependent polarization distribution provides a more feasible method to improve polarization by dropping off positrons with higher θ . For instance, the positrons within 5 mrad, 10 mrad, and 20 mrad, have a longitudinal polarization degree of 48.3%, 46.0%, and 38.7%, respectively. The small emittance ($\sim 0.02 \text{ mm mrad}$) is favorable for experimental operations such as beam injection [61].

The positrons have transverse polarization component P_{\perp} directed radially pointing to the center of the beam-center axis, see Figs.2(c). P_{\perp} presents an angle dependence as well, i.e. $P_{\perp} > 0$ for $\theta_y > 0$, $P_{\perp} < 0$ for $\theta_y < 0$, and the amplitude $|P_{\perp}|$ increasing with the growing of $|\theta_y|$ from 0 to 80%, see see Figs.2(d). The radially polarized positron can be used as transversely polarized positrons by collecting positrons in a certain angle. The controlled transverse polarization would be useful for testing detailed structure of the W^0 coupling. [62].

The reason for generating polarized positrons is analyzed in Fig.3. Processes of photon emission from NCS and pair production from NBW are investigated separately in Figs.3(a) and 3(b). Summing up the final spin states, the analytical

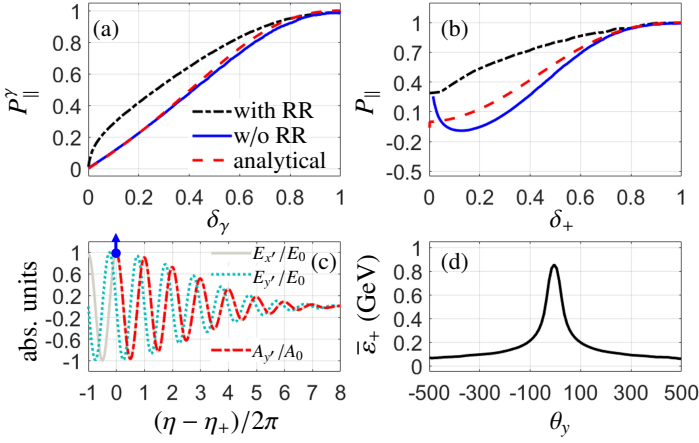


FIG. 3. (a) Circular polarization of photons $P_{\parallel}^{\gamma} = -\bar{\xi}_2$ vs the energy ratio parameter $\delta_{\gamma} = \omega_{\gamma}/\varepsilon_i$, from NCS; (b) Longitudinal polarization of positrons P_{\parallel} vs the energy ratio parameter $\delta_{+} = \varepsilon_{+}/\omega_{\gamma}$, from NBW of an initial photon beam with $\omega_{\gamma} = 10$ GeV; calculated numerically including (black-dash-dotted) or excluding radiation reaction (RR) effect (blue-solid, using the instantaneous $\chi_{e,\gamma}$ parameter), and analytically (red-dashed, employing the constant average value of $\chi_e = 0.97$ or $\chi_{\gamma} = 4.45$). The other parameters are the same with those in Fig.2. (c) Normalized field components of $E_{x'}$ (grey-solid), $E_{y'}$ (cyan-dotted) and vector potential $A_{y'}$ (red-dash-dotted), vs laser phase $\eta - \eta_{+}$, with a positron created at η_{+} (marked with blue point). The blue arrow represents the spin is antiparallel to $\hat{\mathbf{e}}_{y'}$. (d) Average energy $\bar{\varepsilon}_{+}$ vs θ_{γ} , for positrons into $|\theta_{\gamma}| \leq 20$ mrad. (c) and (d) refer to the simulation case in Fig.2.

estimations on circular polarization of photons and longitudinal polarization of positrons read,

$$\xi_2 = P_{\parallel}^i \frac{-u \text{Int} K_{\frac{1}{3}}(u') + u(2+u)K_{\frac{2}{3}}(u')}{-(1+u)\text{Int} K_{\frac{1}{3}}(u') + 2(1+u+u^2/2)K_{\frac{2}{3}}(u')}, \quad (4)$$

$$P_{\parallel} = -\xi_2 \frac{\omega_{\gamma}/\varepsilon_{+} \text{Int} K_{\frac{1}{3}}(\rho) + (\varepsilon_{+}^2 - \varepsilon_{-}^2)/(\varepsilon_{+}\varepsilon_{-})K_{\frac{1}{3}}(\rho)}{(\omega_{\gamma}^2/(\varepsilon_{+}\varepsilon_{-}) - 2)K_{\frac{2}{3}}(\rho) + \text{Int} K_{\frac{1}{3}}(\rho) - \xi_3 K_{\frac{2}{3}}(\rho)}, \quad (5)$$

where, P_{\parallel}^i is the initial electron polarization. The numerical results excluding RR effect, in Figs.3(a) and 3(b), are in coincidence with the analytical ones, with differences mainly coming from the variety of χ_e (χ_{γ}) for photons (positrons) created at diverse points in a laser pulse, and (for Fig.3(b)) from the asymmetry of electromagnetic field experienced by positrons. When radiation reaction is included, electron (positron) loses energy rapidly. The overlapping of photons emitted by electrons with lower energy ($\varepsilon_i < \varepsilon_i$) at higher δ_{γ}^i (i.e., higher P_{\parallel}^{γ}), with photons emitted by electrons with ε_i at δ_{γ}^i , at the condition of $\delta_{\gamma}^i \varepsilon_i = \delta_{\gamma}^j \varepsilon_j$, leads to a higher numerical polarization in the low energy part of $\delta_{\gamma} \ll 1$, in Fig.3(a). Similarly, the overlapping of positrons created at higher δ_{+}^i (i.e., higher P_{\parallel}) experienced more energy-loss $\Delta \varepsilon_{+}^i$, with positrons created at lower δ_{+}^j experienced less energy-loss $\Delta \varepsilon_{+}^j$, at the condition of $\delta_{+}^i \omega_{\gamma} - \Delta \varepsilon_{+}^i = \delta_{+}^j \omega_{\gamma} - \Delta \varepsilon_{+}^j$, results in a higher numerical polarization in the low energy part of $\delta_{+} \ll 1$, in Fig.3(b). Above all, with helicity transferred from initial electron to photon, then to pair, we acquire the longitudinally polarized positrons in Fig.2. The circular polarization of photon (positron) is pro-

portional to its energy, and could approach 100% as ω_{γ} (ε_{+}) gets close to ε_i (ω_{γ}). Intuitively, the simultaneous energy and helicity transferring, from parent particle to new-born particle, causes the fact that higher helicity transfer efficiency would be accompanied by higher energy transfer efficiency.

When a $e^{+}e^{-}$ pair is created at laser phase η_{+} , the final transverse momentum of the positron is $\mathbf{p}_{\perp}^f \approx \mathbf{p}_{\perp}^i - e\mathbf{A}(\eta_{+})$, where \mathbf{p}_{\perp}^i is the momentum inherited from the parent photon, and $\mathbf{A}(\eta_{+})$ is the vector potential at production point. Since \mathbf{p}_{\perp}^i is arbitrary due to the stochastic effects, $\mathbf{p}_{\perp}^f \approx 0$, and consequently the final transverse momenta of positrons should be $\mathbf{p}_{\perp}^f \approx -e\mathbf{A}(\eta_{+})$. For simplicity, we rotate the laboratory coordinate system with respect to instantaneous electromagnetic field, such that $E_{x'} = E_0$, $E_{y'} = 0$, as shown in Fig. 3(c). In the new coordinate system, the final transverse momentum of a positron is antiparallel to the instantaneous $\hat{\mathbf{e}}_{y'}$. Since the pairs are mainly created by energetic photons with longitudinal polarization [50], the transverse polarization arises from the second term in Eq. (3), i.e. $K_{\frac{1}{3}}(\rho)\omega/\varepsilon_{+}\hat{\mathbf{e}}_{y'}$, which also indicates polarization degree $|P_{\perp}|$ inversely proportional to energy. Therefore, positrons are produced with \mathbf{p}_{\perp}^f antiparallel and P_{\perp} parallel to $\hat{\mathbf{e}}_{y'}$ with the rotating of $\hat{\mathbf{e}}_{y'}$, i.e. the positrons are polarized radially, as shown in Fig. 3(c). Meanwhile, as deflection angle $\theta = p_{\perp}/p_{\parallel} \sim 1/\gamma_{e+}$, positrons with higher energy move at smaller deflection angles, as shown in Fig.3(d). Above all, positrons moving closer to axis own higher energy, larger P_{\parallel} but smaller P_{\perp} , as shown in Fig.2(d).

The impacts of laser and electron beam parameters on the production of polarized positrons are investigated in [50]. The polarization of the produced LSP positrons is robust against the variation of pulse duration $\tau(3 - 8T_0)$ and peak intensity $a_0(50\sqrt{2} - 100\sqrt{2})$ of the laser pulse, and initial average kinetic energy $\varepsilon_i(5 - 10\text{GeV})$, angular divergence (0.2-5 mrad) and energy spread (0.06-0.2) of the electron beam. The scheme works very well even for a long electron bunch ($L_e = 100\lambda_0$). Generally speaking, larger a_0 , τ and ε_i are conducive to higher yield and energy of photons emitted and positrons created, as $N_{e+} \propto N_{\gamma} \sim \alpha a_0 \tau / T_0$ and $\varepsilon_{+} \sim \omega_{\gamma} \sim \chi_e \varepsilon_i \sim 10^{-6} a_0 \varepsilon_i^2 / m$ [42, 43]. However, since large χ_e causes strong radiation loss and depolarization [45], a trade off exists for a_0, τ and ε_i .

In conclusion, we have proposed a novel method on production of a highly polarized intense ultrarelativistic positron beam via PW laser pulses available recently, with the help of a newly developed Monte Carlo method. In a feasible scheme with a seed electron beam with polarization degree 80%, density $10^8/\text{bunch}$ and kinetic energy 10 GeV [21, 57], a high-quality positron beam can be generated with polarization degree 40%, angle range 5 mrad, density $10^6/\text{bunch}$ and average energy 1.4 GeV. Given a possible ultrahigh-charge (~ 100 nC [38]) of electron beams, a positron beam density of $10^9 \sim 10^{10}/\text{bunch}$ is foreseeable. The yield and angular divergence of positron beam is increased and decreased, respectively, by orders with respected to the current available ones, making it a promising alternative source for future experimental facilities in high-energy physics, such as ILC. The unavoidable wide energy spread (~ 300 MeV) could be remedied by post-acceleration, e.g. to less than 0.1% at

500 GeV. Moreover, the positron beam has a high flux up to $\sim 10^{19} e^+/s$ thanks to the ultrashort duration ($L_e \simeq 20$ fs), which is favorable for probe [63] along with a potential for ultrafast diagnosis.

Acknowledgement: The authors thank Y.-T. Li and K. Z.

Hatsagortsyan for helpful discussion. This work is supported by the National Natural Science Foundation of China (Grants Nos. 11804269 and Nos. 11775302), the National Key R&D Program of China (Grant No. 2018YFA0404801), and the Strategic Priority Research Program of Chinese Academy of Sciences (Grant No. XDA01020304).

-
- [1] D. W. Gidley, A. R. Köymen, and T. Weston Capehart, “Polarized low-energy positrons: A new probe of surface magnetism,” *Phys. Rev. Lett.* **49**, 1779–1783 (1982).
- [2] J. Van House and P. W. Zitzewitz, “Probing the positron moderation process using high-intensity, highly polarized slow-positron beams,” *Phys. Rev. A* **29**, 96–105 (1984).
- [3] A. Rich, J. Van House, D. W. Gidley, and R. S. Conti, “Spin-polarized low-energy positron beams and their applications,” *Appl. Phys. A* **43**, 275 (1987).
- [4] L. Elouadrhiri, T. A. Forest, J. Grames, W. Melnitchouk, and E. Voutier, “Proceedings of the international workshop on positrons at jefferson lab,” *AIP Conf. Proc.* **1160** (2009).
- [5] A. V. Subashiev, Yu. P. Yashin, J. E. Clendenin, and Yu. A. Mamaev, “Spin polarized electrons: Generation and applications,” *Phys. Low Dimens. Struct.* **1** (1998), [SLAC PUB 8035 (1998)].
- [6] G. Moortgat-Pick, T. Abe, G. Alexander, B. Ananthanarayan, A.A. Babich, V. Bharadwaj, D. Barber, A. Bartl, A. Brachmann, S. Chen, J. Clarke, J.E. Clendenin, J. Dainton, K. Desch, M. Diehl, B. Dobos, T. Dorland, H.K. Dreiner, H. Eberl, J. Ellis, K. Flttmann, H. Fraas, F. Franco-Solova, F. Franke, A. Freitas, J. Goodson, J. Gray, A. Han, S. Heinemeyer, S. Hesselbach, T. Hirose, K. Hohenwarter-Sodek, A. Juste, J. Kalinowski, T. Kernreiter, O. Kittel, S. Kraml, U. Langenfeld, W. Majerotto, A. Martinez, H.-U. Martyn, A. Mikhailichenko, C. Milstene, W. Menges, N. Meyners, K. Mnig, K. Moffeit, S. Moretti, O. Nachtmann, F. Nagel, T. Nakanishi, U. Nauenberg, H. Nowak, T. Otori, P. Osland, A.A. Pankov, N. Paver, R. Pitthan, R. Pschl, W. Porod, J. Proulx, P. Richardson, S. Riemann, S.D. Rindani, T.G. Rizzo, A. Schlicke, P. Schler, C. Schwanenberger, D. Scott, J. Sheppard, R.K. Singh, A. Sopczak, H. Spiesberger, A. Stahl, H. Steiner, A. Wagner, A.M. Weber, G. Weiglein, G.W. Wilson, M. Woods, P. Zerwas, J. Zhang, and F. Zomer, “Polarized positrons and electrons at the linear collider,” *Phys. Rep.* **460**, 131 – 243 (2008).
- [7] Ties Behnke, James E. Brau, Brian Foster, Juan Fuster, Mike Harrison, James McEwan Paterson, Michael Peskin, Marcel Stanitzki, Nicholas Walker, and Hitoshi Yamamoto, “The international linear collider technical design report - volume 1: Executive summary,” arXiv:1306.6327 [physics.acc-ph] (2013).
- [8] K. Flottman, “Investigations toward the development of polarized and unpolarized high intensity positron sources for linear colliders,” DESY 93-161 November 1993.
- [9] P. W. Zitzewitz, J. C. Van House, A. Rich, and D. W. Gidley, “Spin polarization of low-energy positron beams,” *Phys. Rev. Lett.* **43**, 1281–1284 (1979).
- [10] A. A. Sokolov and I. M. Ternov, *Sov. Phys. Dokl.* **8**, 1203 (1964).
- [11] T. Otori, M. Fukuda, T. Hirose, Y. Kurihara, R. Kuroda, M. Nomura, A. Ohashi, T. Okugi, K. Sakaue, T. Saito, J. Urakawa, M. Washio, and I. Yamazaki, “Efficient propagation of polarization from laser photons to positrons through Compton scattering and electron-positron pair creation,” *Phys. Rev. Lett.* **96**, 114801 (2006).
- [12] G. Alexander, J. Barley, Y. Batygin, S. Berridge, V. Bharadwaj, G. Bower, W. Bugg, F.-J. Decker, R. Dollan, Y. Efremenko, V. Gharibyan, C. Hast, R. Iverson, H. Kolanoski, J. Kovermann, K. Laihem, T. Lohse, K. T. McDonald, A. A. Mikhailichenko, G. A. Moortgat-Pick, P. Pahl, R. Pitthan, R. Pöschl, E. Reinherz-Aronis, S. Riemann, A. Schällicke, K. P. Schüller, T. Schweizer, D. Scott, J. C. Sheppard, A. Stahl, Z. M. Szalata, D. Walz, and A. W. Weidemann, “Observation of polarized positrons from an undulator-based source,” *Phys. Rev. Lett.* **100**, 210801 (2008).
- [13] D. Abbott, P. Adderley, A. Adeyemi, P. Aguilera, M. Ali, H. Areti, M. Baylac, J. Benesch, G. Bosson, B. Cade, A. Camsonne, L. S. Cardman, J. Clark, P. Cole, S. Covert, C. Cuevas, O. Dadoun, D. Dale, H. Dong, J. Dumas, E. Fanchini, T. Forest, E. Forman, A. Freyberger, E. Froidefond, S. Golge, J. Grames, P. Guèye, J. Hansknecht, P. Harrell, J. Hoskins, C. Hyde, B. Josey, R. Kazimi, Y. Kim, D. Machie, K. Mahoney, R. Mammei, M. Marton, J. McCarter, M. McCaughan, M. McHugh, D. McNulty, K. E. Mesick, T. Michaelides, R. Michaels, B. Moffit, D. Moser, C. Muñoz Camacho, J.-F. Muraz, A. Oppen, M. Poelker, J.-S. Réal, L. Richardson, S. Setiniyaz, M. Stutzman, R. Suleiman, C. Tennant, C. Tsai, D. Turner, M. Ungaro, A. Variola, E. Voutier, Y. Wang, and Y. Zhang (PEPPo Collaboration), “Production of highly polarized positrons using polarized electrons at MeV energies,” *Phys. Rev. Lett.* **116**, 214801 (2016).
- [14] S. Corde, K. Ta Phuoc, G. Lambert, R. Fitour, V. Malka, A. Rousse, A. Beck, and E. Lefebvre, “Femtosecond x rays from laser-plasma accelerators,” *Rev. Mod. Phys.* **85**, 1–48 (2013).
- [15] A.P. Potylitsin, “Production of polarized positrons through interaction of longitudinally polarized electrons with thin targets,” *Nucl. Instrum. Methods Phys. Res., Sect. A* **398**, 395 – 398 (1997).
- [16] William H. McMaster, “Matrix representation of polarization,” *Rev. Mod. Phys.* **33**, 8–28 (1961).
- [17] V. A. Baskov, “Radiation length of the oriented crystal,” *Bull. Lebedev Phys. Inst.* **42**, 144 (2015).
- [18] Haakon Olsen and L. C. Maximon, “Photon and electron polarization in high-energy bremsstrahlung and pair production with screening,” *Phys. Rev.* **114**, 887–904 (1959).
- [19] James C. Liu, T. Kotseroglou, W. R. Nelson, and D. Schultz, “Polarization study for nlc positron source using egs4,” SLAC-PUB-8477 June 16 2000.
- [20] Jin Woo Yoon, Cheonha Jeon, Junghoon Shin, Seong Ku Lee, Hwang Woon Lee, Il Woo Choi, Hyung Taek Kim, Jae Hee Sung, and Chang Hee Nam, “Achieving the laser intensity of $5.5 \times 10^{22} \text{ W/cm}^2$ with a wavefront-corrected multi-pw laser,” *Opt. Express* **27**, 20412–20420 (2019).
- [21] Meng Wen, Matteo Tamburini, and Christoph H. Keitel, “Polarized laser-wakefield-accelerated kiloampere electron beams,” *Phys. Rev. Lett.* **122**, 214801 (2019).
- [22] Yan-Fei Li, Rashid Shaisultanov, Karen Z. Hatsagortsyan, Feng Wan, Christoph H. Keitel, and Jian-Xing Li, “Ultra-relativistic electron-beam polarization in single-shot interaction with an ultra-intense laser pulse,” *Phys. Rev. Lett.* **122**, 154801 (2019).

- [23] Daniel Seipt, Dario Del Sorbo, Christopher P. Ridgers, and Alec G. R. Thomas, “Ultrafast polarization of an electron beam in an intense bichromatic laser field,” *Phys. Rev. A* **100**, 061402 (2019).
- [24] Yitong Wu, Liangliang Ji, Xuesong Geng, Qin Yu, Nengwen Wang, Bo Feng, Zhao Guo, Weiqing Wang, Chengyu Qin, Xue Yan, Lingang Zhang, Johannes Thomas, Anna Hützen, Alexander Pukhov, Markus Büscher, Baifei Shen, and Ruxin Li, “Polarized electron acceleration in beam-driven plasma wake-field based on density down-ramp injection,” *Phys. Rev. E* **100**, 043202 (2019).
- [25] Huai-Hang Song, Wei-Min Wang, Jian-Xing Li, Yan-Fei Li, and Yu-Tong Li, “Spin-polarization effects of an ultrarelativistic electron beam in an ultraintense two-color laser pulse,” *Phys. Rev. A* **100**, 033407 (2019).
- [26] Yan-Fei Li, Rashid Shaisultanov, Yue-Yue Chen, Feng Wan, Karen Z. Hatsagortsyan, Christoph H. Keitel, and Jian-Xing Li, “Polarized ultrashort brilliant multi-gev γ rays via single-shot laser-electron interaction,” *Phys. Rev. Lett.* **124**, 014801 (2020).
- [27] Yue-Yue Chen, Pei-Lun He, Rashid Shaisultanov, Karen Z. Hatsagortsyan, and Christoph H. Keitel, “Polarized positron beams via intense two-color laser pulses,” *Phys. Rev. Lett.* **123**, 174801 (2019).
- [28] Feng Wan, Rashid Shaisultanov, Yan-Fei Li, Karen Z. Hatsagortsyan, Christoph H. Keitel, and Jian-Xing Li, “Ultrarelativistic polarized positron jets via collision of electron and ultraintense laser beams,” *Phys. Lett. B* **800**, 135120 (2020).
- [29] B. King and N. Elkina, “Vacuum birefringence in high-energy laser-electron collisions,” *Phys. Rev. A* **94**, 062102 (2016).
- [30] D. Del Sorbo, D. Seipt, T. G. Blackburn, A. G. R. Thomas, C. D. Murphy, J. G. Kirk, and C. P. Ridgers, “Spin polarization of electrons by ultraintense lasers,” *Phys. Rev. A* **96**, 043407 (2017).
- [31] E. Esarey, C. B. Schroeder, and W. P. Leemans, “Physics of laser-driven plasma-based electron accelerators,” *Rev. Mod. Phys.* **81**, 1229–1285 (2009).
- [32] Gerard A. Mourou, Toshiki Tajima, and Sergei V. Bulanov, “Optics in the relativistic regime,” *Rev. Mod. Phys.* **78**, 309–371 (2006).
- [33] Andrea Macchi, Marco Borghesi, and Matteo Passoni, “Ion acceleration by superintense laser-plasma interaction,” *Rev. Mod. Phys.* **85**, 751–793 (2013).
- [34] J. Ferri, S. Corde, A. Döpp, A. Lifschitz, A. Doche, C. Thauray, K. Ta Phuoc, B. Mahieu, I. A. Andriyash, V. Malka, and X. Davoine, “High-brilliance betatron γ -ray source powered by laser-accelerated electrons,” *Phys. Rev. Lett.* **120**, 254802 (2018).
- [35] Wei-Min Wang, Zheng-Ming Sheng, Paul Gibbon, Li-Ming Chen, Yu-Tong Li, and Jie Zhang, “Collimated ultrabright gamma rays from electron wiggling along a petawatt laser-irradiated wire in the qed regime,” *Proc. Natl. Acad. Sci.* **115**, 9911–9916 (2018).
- [36] O. Lundh, J. Lim, C. Rechatin, L. Ammoura, A. Ben-Ismael, X. Davoine, G. Gallot, J.-P. Goddet, E. Lefebvre, V. Malka, and J. Faure, “Few femtosecond, few kiloampere electron bunch produced by a laserplasma accelerator,” *Nat. Phys.* **7** (2011).
- [37] R. Weingartner, S. Raith, A. Popp, S. Chou, J. Wenz, K. Khrennikov, M. Heigoldt, A. R. Maier, N. Kajumba, M. Fuchs, B. Zeitler, F. Krausz, S. Karsch, and F. Grüner, “Ultralow emittance electron beams from a laser-wakefield accelerator,” *Phys. Rev. ST Accel. Beams* **15**, 111302 (2012).
- [38] Yong Ma, Jiarui Zhao, Yifei Li, Dazhang Li, Liming Chen, Jianxun Liu, Stephen J. D. Dann, Yanyun Ma, Xiaohu Yang, Zheyi Ge, Zhengming Sheng, and Jie Zhang, “Ultrahigh-charge electron beams from laser-irradiated solid surface,” *Proc. Natl. Acad. Sci.* **115**, 6980–6985 (2018).
- [39] Xing Long Zhu, Tong-Pu Yu, Zheng-Ming Sheng, Yan Yin, Ion Cristian Edmond Turcu, and Alexander Pukhov, “Dense gev electronpositron pairs generated by lasers in near-critical-density plasmas,” *Nat. Comm.* **7**, 13686.
- [40] K.-H. Steffens, H.G. Andresen, J. Blume-Werry, F. Klein, K. Aulenbacher, and E. Reichert, “A spin rotator for producing a longitudinally polarized electron beam with mami,” *Nucl. Instrum. Methods Phys. Res., Sect. A* **325**, 378 – 383 (1993).
- [41] Jean Buon and Klaus Steffen, “Hera variable-energy mini spin rotator and head-on ep collision scheme with choice of electron helicity,” *Nucl. Instrum. Methods Phys. Res., Sect. A* **245**, 248 – 261 (1986).
- [42] A. Di Piazza, C. Müller, K. Z. Hatsagortsyan, and C. H. Keitel, “Extremely high-intensity laser interactions with fundamental quantum systems,” *Rev. Mod. Phys.* **84**, 1177–1228 (2012).
- [43] V. I. Ritus, *J. Sov. Laser Res.* **6**, 497 (1985).
- [44] M. B. Plenio and P. L. Knight, “The quantum-jump approach to dissipative dynamics in quantum optics,” *Rev. Mod. Phys.* **70**, 101–144 (1998).
- [45] V. N. Baier, V. M. Katkov, and V. M. Strakhovenko, *Electromagnetic Processes at High Energies in Oriented Single Crystals* (World Scientific, Singapore, 1998).
- [46] C.P. Ridgers, J.G. Kirk, R. Ducloux, T.G. Blackburn, C.S. Brady, K. Bennett, T.D. Arber, and A.R. Bell, “Modelling gamma-ray photon emission and pair production in high-intensity laser-matter interactions,” *J. Comput. Phys.* **260**, 273 – 285 (2014).
- [47] N. V. Elkina, A. M. Fedotov, I. Yu. Kostyukov, M. V. Legkov, N. B. Narozhny, E. N. Nerush, and H. Ruhl, “Qed cascades induced by circularly polarized laser fields,” *Phys. Rev. ST Accel. Beams* **14**, 054401 (2011).
- [48] A. Gonoskov, S. Bastrakov, E. Efimenko, A. Ilderton, M. Marklund, I. Meyerov, A. Muraviev, A. Sergeev, I. Surmin, and E. Wallin, “Extended particle-in-cell schemes for physics in ultrastrong laser fields: Review and developments,” *Phys. Rev. E* **92**, 023305 (2015).
- [49] Users Manual of CAIN Version 2.42, <http://lcddev.kek.jp/~yokoya/CAIN/>.
- [50] Supplemental Materials, For details on the applied theoretical model, and simulated results for other laser and electron parameters.
- [51] M. Kh. Khokonov and I. Z. Bekulova, “Length of formation of processes in a constant external field at high energies,” *Tech. Phys.* **55**, 728–731 (2010).
- [52] V. B. Berestetskii, E. M. Lifshitz, and L. P. Pitaevskii, *Quantum Electrodynamics* (Pergamon, Oxford, 1982).
- [53] B. King, N. Elkina, and H. Ruhl, “Photon polarization in electron-seeded pair-creation cascades,” *Phys. Rev. A* **87**, 042117 (2013).
- [54] Feng Wan, Yu Wang, Ren-Tong Guo, Yue-Yue Chen and Rashid Shaisultanov, Zhong-Feng Xu, Karen Z. Hatsagortsyan, Christoph H. Keitel, and Jian-Xing Li, “High-energy γ -photon polarization in nonlinear breit-wheeler pair production and γ -polarimetry,” arXiv:2002.10346 (2020).
- [55] V. Bargmann, Louis Michel, and V. L. Telegdi, “Precession of the polarization of particles moving in a homogeneous electromagnetic field,” *Phys. Rev. Lett.* **2**, 435–436 (1959).
- [56] Yousef I. Salamin, Guido R. Mocken, and Christoph H. Keitel, “Electron scattering and acceleration by a tightly focused laser beam,” *Phys. Rev. ST Accel. Beams* **5**, 101301 (2002).
- [57] A. J. Gonsalves, K. Nakamura, J. Daniels, C. Benedetti, C. Pieronek, T. C. H. de Raadt, S. Steinke, J. H. Bin, S. S. Bulanov, J. van Tilborg, C. G. R. Geddes, C. B. Schroeder, Cs.

- Tóth, E. Esarey, K. Swanson, L. Fan-Chiang, G. Bagdasarov, N. Bobrova, V. Gasilov, G. Korn, P. Sasorov, and W. P. Leemans, “Petawatt laser guiding and electron beam acceleration to 8 gev in a laser-heated capillary discharge waveguide,” *Phys. Rev. Lett.* **122**, 084801 (2019).
- [58] W. P. Leemans, A. J. Gonsalves, H.-S. Mao, K. Nakamura, C. Benedetti, C. B. Schroeder, Cs. Tóth, J. Daniels, D. E. Mittelberger, S. S. Bulanov, J.-L. Vay, C. G. R. Geddes, and E. Esarey, “Multi-gev electron beams from capillary-discharge-guided sub-petawatt laser pulses in the self-trapping regime,” *Phys. Rev. Lett.* **113**, 245002 (2014).
- [59] A. Apyan, R. O. Avakian, B. Badelek, S. Ballestrero, C. Biino, I. Birol, P. Cenci, S. H. Connell, S. Eichblatt, T. Fonseca, A. Freund, B. Gorini, R. Groess, K. Ispirian, T. J. Ketel, Yu. V. Kononets, A. Lopez, A. Mangiarotti, B. van Rens, J. P. F. Sell-schop, M. Shieh, P. Sona, V. Strakhovenko, E. Uggerhøj, U. I. Uggerhøj, G. Unel, M. Velasco, Z. Z. Vilakazi, and O. Wessely (NA59 Collaboration), “Coherent bremsstrahlung, coherent pair production, birefringence, and polarimetry in the 20–170 gev energy range using aligned crystals,” *Phys. Rev. ST Accel. Beams* **11**, 041001 (2008).
- [60] Ralph Dollan, Karim Laihem, and Andreas Sch’alick, “Monte-carlo-based studies of a polarized positron source for international linear collider (ilc),” *Nucl. Instrum. Methods Phys. Res., Sect. A* **559**, 185 – 189 (2006).
- [61] X. Artru, R. Chehab, M. Chevallier, V.M. Strakhovenko, A. Variola, and A. Vivoli, “Polarized and unpolarized positron sources for electronpositron colliders,” *Nucl. Instrum. Methods Phys. Res., Sect. B* **266**, 3868 – 3875 (2008).
- [62] Robert Budny, “Weak effects in annihilations producing spin-1/2 and spin-0 particle pairs,” *Phys. Rev. D* **14**, 2969–2989 (1976).
- [63] Nikolay Djourellov, Andreea Oprisa, and Victor Leca, “Project for a source of polarized slow positrons at eli-np,” in *Positron Annihilation - ICPA-17*, Defect and Diffusion Forum, Vol. 373 (Trans Tech Publications Ltd, 2017) pp. 57–60.